ARTICLES

Hessian Biased Force Field for Polysilane Polymers

Charles B. Musgrave, Siddharth Dasgupta, and William A. Goddard III*

Materials and Process Simulation Center (MSC), Beckman Institute (139-74), Division of Chemistry and Chemical Engineering (CN 9041), California Institute of Technology, Pasadena, California 91125

Received: January 30, 1995; In Final Form: May 16, 1995[⊗]

We report a force field (FF) suitable for molecular dynamics simulations of polysilane polymers. This FF, denoted MSXX, was developed using the Hessian biased method to describe accurately the vibrational states, the *ab initio* torsional potential energy surface, and the *ab initio* electrostatic charges of polysilane oligomers. This MSXX FF was used to calculate various spectroscopic and mechanical properties of the polysilane crystal. Stress−strain curves and surface energies are reported. Gibbs molecular dynamics calculations (Nosè, Rahman−Parrinello) were used to predict various materials properties at higher temperatures. Phonon dispersion curves and elastic constants were calculated at various temperatures. Although this polymer is of increasing industrial interest, we could find no experimental data with which to compare these predictions.

I. Introduction

Polysilane polymers, $-[-SiH_2-]_n-$ denoted herein as P(SiH), have become of significant interest. The substituted derivatives of P(SiH) can be used as precursors to SiC ceramics, as nonlinear optical materials, as semiconducting polymers, and as photoresists.[1] The polysilane polymers are amorphous, and their structural, physical, and electronic properties are not well characterized.[2−5] In order to predict such properties, we have developed a force field (FF) expected to be accurate for predicting structural, mechanical, vibrational, and thermodynamic properties.

Section II develops the FF, and section III applies this FF to the prediction of various properties for P(SiH) oligomers. The properties of P(SiH) crystals are predicted in section IV.

II. Development of the MSXX Force Field

II.A. Introduction. The general form of the FF is taken as

$$E = E^{val} + E^{Q} + E^{vdw} \tag{1}$$

Here the Coulomb term

$$E^{Q} = C_{coul}\sum_{i>j}\frac{q_i q_j}{R_{ij}} \tag{2}$$

represents the electrostatic interactions between partial charges on the various atoms ($C_{coul} = 332.0637$ converts units so that the R is in angstroms and E^{Q} is in kilocalories per mole), the van der Waals (vdW) term

$$E^{vdw} = \sum_{i>j} E_{ij}^{vdw}(R_{ij}) \tag{3}$$

represents the long-range attraction (London dispersion) and short-range repulsion (Pauli orthogonalization of nonbonded electrons), and the valence term

$$E^{val} = E^{bond} + E^{angle} + E^{cross} + E^{torsion} \tag{4}$$

represents all terms involving bonds between atoms and coupling behavior of these bonds.

Our general approach to developing force fields is to emphasize the use of accurate quantum chemical calculations on model systems. Thus, the atomic charges [for E^{Q}] and the torsional potentials about single bonds [for $E^{torsion}$] are taken directly from Hartree−Fock (HF) calculations using good basis sets. The force constant parameters important in describing valence interactions (E^{bond}, E^{angle}, E^{cross}) are taken from the Hessian (second derivative of energy with respect to atomic coordinates) calculated from HF wave functions. However, the eigenfunctions of this Hessian are modified [the Hessian biased[6] FF, HBFF] since HF vibrational frequencies are too high. Herein we derive the HBFF for P(SiH) using the following model systems: SiH_4, Si_2H_6, Si_3H_8, n-Si_4H_{10}. Only the vdW terms, (3), are not based on HF calculations. The vdW parameters for Si and H were obtained from the Dreiding FF[7] which were based on fits to experimental structural data for simple solids and on extrapolations.

On the basis of these individual HBFF we determine a final FF, denoted MSXX, recommended for all silane systems, including P(SiH). Thus the discussions use HBFF to refer to the FF for any particular molecule and MSXX to denote the final recommended FF (based mostly on Si_4H_{10}).

II.B. Calculations. For each model system we carried out HF calculations using the 6-31G** basis set. The geometry was optimized at the HF level (using Gaussian 92[8] and PS-GVB[9]), and this geometry was used in determining the FF. With comparison to experiment the HF geometry leads to errors of about 0.02 Å in Si−Si distances, 0.01 Å in Si−H distances, and 0.5° in bond angles (see Table 1).

We use the potential derived charges (PDQ) from HF as the partial atomic charges.[10] PDQ are derived by (i) calculating the electron density distribution, $\varrho(r)$, from the HF wave function, (ii) using $\varrho(r)$ to calculate the electrostatic potential on a set of grid points around the molecule,

* To whom correspondence should be addressed.

[⊗] Abstract published in *Advance ACS Abstracts,* August 15, 1995.

0022-3654/95/2099-13321$09.00/0

TABLE 1: Structural Parameters (Distances in angstroms; angles in degrees)

molecule	feature[b,e]	MSXX[c] FF	HF/6-31G**	n-Si_4H_{10} FF[d]	expt[a]
SiH_3	SiH	1.476	1.476		
	HSiH	111.01	111.01		110.6
SiH_4	SiH	1.476	1.476	1.476	1.481
Si_2H_6	SiSi	2.353	2.353	2.356	2.331
	HSi	1.479	1.479	1.479	1.492
	HSiSi	110.35	110.35	110.50	110.3
Si_3H_8	$SiSi_c$	2.358	2.357	2.351	
	H_cSi_c	1.482	1.482	1.482	
	$H_{ip}Si$	1.479	1.478	1.477	
	$H_{op}Si$	1.479	1.479	1.478	
	$SiSi_cSi$	112.73	112.56	108.83	
	$H_{ip}SiSi_c$	110.74	110.69	110.84	
	$H_{op}SiSi_c$	110.17	110.16	109.75	
	H_cSi_cSi	109.07	109.12	109.98	
	$H_{op}SiSi_cSi$	59.77	59.77	59.65	
n-Si_4H_{10}	$SiSi_c$	2.358	2.357		
	Si_cSi_c	2.362	2.361		
	H_cSi_c	1.481	1.482		
	$H_{ip}Si$	1.480	1.479		
	$H_{op}Si$	1.479	1.479		
	$SiSi_cSi_c$	113.06	112.73		
	$H_{ip}SiSi_c$	110.86	110.73		
	$H_{op}SiSi$	110.01	110.08		
	H_cSi_cSi	109.22	109.30		
	$H_{op}SiSi_cSi_c$	59.76	59.79		
	$H_cSi_cSi_cSi$	58.32	58.48		

[a] References 15 and 16. [b] Si_c and H_c denote atoms of SiH_2 groups. These are used in the P(SiH) FF. [c] Separate FF for each molecule parameters in Table 6a. [d] Using the MSXX FF of n-Si_4H_{10} to calculate the structure of the other molecules. [e] ip and op denote in-plane and out-of-plane hydrogens, respectively.

$$V^{HF}(R_g) = \int d^3r \frac{\varrho(r)}{|R - R_g|^j} \tag{5}$$

and (iii) determining the set of atomic point charges on the various atoms to optimally fit this electrostatic potential,

$$V^{Q}(R_g) = \sum_i \frac{q_i}{|R_i - R_g|} \approx V^{HF}(R_g) \tag{6}$$

at grid points outside the van der Waals (vdW) radii. The PDQ charges (from Gaussian 92) as well as Mulliken populations are shown in Table 2. On the basis of these calculations we recommend in Table 2 the charges for P(SiH) chains.

II.C. Biased Hessian Method. From *ab initio* HF wave functions we calculate[8] a full Hessian

$$H^{HF}_{\alpha i;\beta j} = \frac{\partial^2 E^{HF}}{\partial R_{\alpha i}\, \partial R_{\beta j}} \tag{7}$$

where $R_{\alpha i}$ is the α component (x, y, z) of the coordinates of atom i. After mass weighting,

$$\bar{H}^{HF}_{\alpha i,\beta j} = \frac{1}{[M_i M_j]^{1/2}} H^{HF}_{\alpha i,\beta j} \tag{8}$$

the vibrational modes $\{\mathbf{U}_i^{HF}\}$ and vibrational frequencies $\{\nu_i^{HF}\}$ are obtained by solving

$$\bar{\mathbf{H}}^{HF}\mathbf{U}_i^{HF} = \mathbf{U}^{HF}\lambda_i^{HF} \tag{9a}$$

where

$$\lambda_i^{HF} = (C_{freq}\nu_i^{HF})^2 \tag{9b}$$

and $C_{freq} = 108.5913$ converts units so that energies are in kilocalories per mole, distances are in angstroms, frequencies are in cm^{-1}, and masses are in atomic mass units (C^{12} has mass = 12.0000 amu). This Hessian provides $g(g+1)/2$ independent pieces of information [666 for Si_4H_{10}], where $g = 3N - 6$ is the number of degrees of freedom. These constraints are sufficient for determining the FF. In contrast, fitting just the frequencies leads to only g conditions [36 for n-Si_4H_{10}]. However, at the HF level the calculated frequencies, ν_i^{HF}, are 10−20% too high. This led to the development of the Hessian biased method[6] for FF parametrization in which the FF is fit to the biased Hessian

$$\mathbf{H}^{HB} = \mathbf{U}^{HF}\lambda^{exp}\tilde{\mathbf{U}}^{HF} \tag{10}$$

where $\tilde{\mathbf{U}}$ is the transpose and λ^{exp} is the diagonal matrix based on experimental frequencies

$$\lambda_i^{exp} = (C_{freq}\nu_i^{exp})^2 \tag{11}$$

This Hessian has the property that, $\mathbf{H}^{HB}\mathbf{U}^{HF} = \mathbf{U}^{HF}\lambda^{exp}$; that is, the eigenvalues match experiment while the eigenfunctions match HF theory. Thus, $\mathbf{H}^{HB}$ has the best available information on the vibrational modes. Also, since $\mathbf{H}^{HB}$ is a full symmetric $3N \times 3N$ matrix, the use of the nonzero off-diagonal terms provides many more constraints than can be obtained by fitting to the experimental frequencies alone (diagonal elements of the λ^{exp} matrix).

In general the optimum geometry at the HF level differs slightly from experiment, raising the question of which structure to use in (10). We use the structures optimized at the Hartree−Fock level of theory. Previously[6,11a] we advocated the use of the experimental structure for determining force constants from the *ab initio* calculations, primarily because the internuclear separations (which strongly affect the Hessian) reflect the experimental system. However, in molecules with low frequency torsions, a slight difference in structure can cause a noticeable rotational contamination of the torsional modes. Since we want to use frequency scaling parameters to compare various molecules, it is better to derive the frequencies for all molecules at the *ab initio* minima (rather than at the experimental minimum for molecules where experimental geometries are available and the *ab initio* minimum for those where experimental geometries are not available). Fortunately, as indicated in Table 1, the differences between the *ab initio* and experimental geometries are small.

II.D. Scaling of *ab Initio* Frequencies. To obtain the most accurate FF, we prefer to use in HBFF the most complete set of frequencies from experiment (excepting the torsional modes, as discussed in section II.E). For both Si_3H_8 and n-Si_4H_{10} the set of experimental frequencies is incomplete. In order to estimate the experimentally undetermined modes, we scale the *ab initio* frequencies for these modes using scale factors (the ratio of the experimental frequency to the *ab initio* frequency) obtained from the observed modes of these and related molecules. This is similar in spirit to Pulay's "Scaled Quantum Mechanical Force Field".[11b] This works well because the scale factor is nearly constant within a particular class of vibrations, even between different molecules. For example, it is 0.901 ± 0.016 for the SiH bending modes of Si_3H_8. (A further refinement is to calculate separate average scales for the rocking, wagging, and scissor SiH bending modes.) Table 4 shows the scale factors derived for each molecule. Because the scales vary little from molecule to molecule, the scaling procedure can be applied even to molecules with no experimental frequencies. Table 5 shows the Si_5H_{12} scaled frequencies (using values from

TABLE 2: Atomic Charges (electron units) from HF Calculations on Linear (All Trans) Chains[a]

	Si_2H_6		Si_3H_8		Si_4H_{10}		Si_5H_{12}	
atom[b]	PDQ	Mulliken	PDQ	Mulliken	PDQ	Mulliken	PDQ	Mulliken
Si $(SiH_2)'$							0.2971	0.2878
H $(SiH_2)'$							−0.1485	−0.1508
Si (SiH_2)			0.1550	0.2287	0.2211	0.2565	0.2287	0.2617
H (SiH_2)			−0.1042	−0.1491	−0.1274	−0.1501	−0.1260	−0.1495
Si (SiH_3)	0.3936	0.4752	0.4714	0.5096	0.4829	0.5175	0.4494	0.5138
H $(SiH_3)_{ip}$	−0.1312	−0.1584	−0.1369	−0.1567	−0.1458	−0.1569	−0.1370	−0.1570
H $(SiH_3)_{op}$			−0.1424	−0.159	−0.1518	−0.1584	−0.1446	−0.1584

[a] On the basis of these results we recommend the following: (i) $Q_{Si} = 0.30$ and $Q_H = -0.15$ for SiH_2 of P(SiH), (ii) $Q_{Si} = 0.44$ and $Q_H = -0.14$ for terminal SiH_3 groups, and (iii) $Q_{Si} = 0.23$ and $Q_H = -0.125$ for SiH_2 next to a terminal group. [b] Primes signify central SiH_2. ip and op denote in-plane and out-of-plane hydrogens, respectively.

TABLE 3: Torsional Potentials (kcal/mol)

(a) For Si_2H_6[a]

ϕ	HF	MSXX	ϕ	MF	MSXX	ϕ	MF	MSXX
60.000	0.00000	0.00000	30.000	0.47000	0.49150	0.0000	0.97400	0.97290
45.000	0.13500	0.14490	15.000	0.82300	0.83280			

(b) For Si_3H_8 for Various Values of the Two Dihedral Angles, ϕ_1 and ϕ_2[a,b]

	MSXX torsional energies at given ϕ_2					HF torsional energies at given ϕ_2				
ϕ_1/ϕ_2	180	165	150	135	120	180	165	150	135	120
180	0	0.1205	0.4241	0.7504	0.8995	0	0.1150	0.3389	0.6884	0.8161
165	0.1205	0.2478	0.5568	0.8839	1.0278	0.1150	0.2058	0.4897	0.8111	0.9728
150	0.4241	0.5568	0.8734	1.2069	1.3511	0.3389	0.4897	0.8082	1.1716	1.3585
135	0.7504	0.8839	1.2069	1.5505	1.7011	0.6884	0.8111	1.1716	1.5656	1.7533
120	0.8995	1.0278	1.3511	1.7011	1.8601	0.8161	0.9728	1.3586	1.7533	1.9196
105	0.7504	0.8839	1.2069	1.5505	1.7011	0.6884	0.8111	1.1716	1.5656	1.7533
90	0.4241	0.5568	0.8734	1.2069	1.3511	0.3389	0.4897	0.8082	1.1716	1.3585
75	0.1205	0.2478	0.5568	0.8839	1.0278	0.1150	0.2058	0.4897	0.811	0.9727
60	0.0000	0.1205	0.4241	0.7504	0.8995	0.0000	0.1150	0.3389	0.6884	0.8161
45	0.1205	0.2478	0.5568	0.8839	1.0278	0.1150	0.2058	0.4897	0.8111	0.9727
30	0.4241	0.5568	0.8734	1.2069	1.3511	0.3389	0.4897	0.8082	1.1716	1.3585
15	0.7504	0.8839	1.2069	1.5505	1.7011	0.6884	0.8111	1.1716	1.5656	1.7533
0	0.8995	1.0278	1.3511	1.7011	1.8601	1.8161	0.9728	1.3586	1.7533	1.9196

(c) For the Central Torsion Angle of n-Si_4H_{10}[a,c]

ϕ	HF	MSXX	E_{tor}	ϕ	HF	MSXX	E_{tor}	ϕ	HF	MSXX	E_{tor}
0	1.5631	1.5628	0.7189	75	0.1639	0.1504	0.0734	150	0.3190	0.3110	−0.0247
15	1.3380	1.3302	0.6682	90	0.3238	0.3189	−0.0324	165	0.0986	0.0883	0.0018
30	0.8461	0.8345	0.5271	105	0.5261	0.5376	−0.1005	180	0.0000	0.0000	0.0000
45	0.3893	0.3891	0.3455	120	0.6735	0.6458	−0.0657				
60	0.1539	0.1542	0.1891	135	0.5359	0.5478	−0.0787				

[a] All bonds and angles were optimized at each ϕ. E_{FF}^{tor} is described with a single 3-fold term (17) with a barrier $V_3 = 0.94$ kcal/mol (see Table 7a). [b] $E_{tor}^{FF}(\phi)$ is described using the HSiSiH torsion from (a) plus a single 3-fold HSiSiSi torsion with barrier of $V_3 = 0.806$ kcal/mol (see Table 7a). [c] For each ϕ all other structural parameters were optimized (at either the HF or FF level). The $E_{tor}(\phi)$ was described with the HSiSiH and HSiSiSi terms from (a) and (b) plus a three term SiSiSiSi potential (see Table 7a). The last column is the SiSiSiSi torsional potential (after eliminating the other nonbond and valence torsions).

TABLE 4: Scale Factors (Ratio of Experimental Value to HF Value) for Estimating Experimental Frequency from HF Vibrational Frequencies[a]

mode	SiH_4	Si_2H_6	Si_3H_8	n-Si_4H_{10}
SiH stretch	0.9255	0.9113	0.9163	0.9140
	(0.0035)	(0.0215)	(0.0015)	(0.001)
SiH bend	0.9125	0.8972	0.9009	0.9081
	(0.0191)	(0.0126)	(0.0162)	(0.203)
SiSi stretch		0.9100	0.9370	0.9177
			(0.0226)	(0.0055)
SiSiSi bend			1.025	

[a] Standard deviations are in parentheses.

HF in Table 4) and those predicted by the MSXX (from n-Si_4H_{10}). Here the MSXX vibrations differ from the HF scaled values by 13 cm^{-1} (root mean square (rms) error), about the same as for cases where the experiment is available.

Torsions do not follow the same scaling trend as bending and stretching modes. However, we base all torsional parameters on the HF torsion curves rather than on scaled torsional vibrations.

II.E. Potential Energy Surface for Torsions. The distribution of conformations in a polymer and the rates of conformational transitions have a strong effect on the properties (moduli, glass temperature); hence, it is critical that the FF lead to the correct relative energies of the minima (e.g., trans versus gauche) and of the barrier heights between them. Thus, torsional FF parameters are particularly important for describing amorphous polymers. Fitting to the low frequency torsional mode from experiment fits only the curvature near the minimum in this potential. Other local minima (e.g. the gauche conformation in n-butane and its analogues) would not necessarily be accurately fit by this procedure. In many cases, the existence of the molecule in other local minima can be detected experimentally, but frequencies and energies for these states are usually not reliably obtained from experiment. In addition,

TABLE 5: Predicted Vibrational Frequencies (cm^{-1}) for n-Si_5H_{12}[a]

mode	sym	character	MSXX	scaled[b]	HF[c]	MP2[c]
1	B_2	SiSi torsion	24	23	23	52
2	A_2	SiSi torsion	26	26	26	43
3	A_1	SiSiSi bend	47	45	49	56
4	A_2	SiH_3 torsion	93	89	89	111
5	B_2	SiH_3 torsion	95	90	90	112
6	B_1	SiSiSi bend	104	105	115	112
7	A_1	SiSiSi bend[d]	138	137	131	124
8	B_2	SiH_2 rock	303	301	331	300
9	A_2	SiH_2 rock	322	321	353	329
10	A_1	SiSi stretch	366	366	399	383
11	B_2	twist−rock	379	376	414	391
12	B_1	SiSi stretch	392	397	433	414
13	A_1	SiSi stretch	446	441	482	463
14	A_2	SiSi stretch	457	464	506	483
15	B_1	twist	464	461	508	487
16	B_1	SiH_3 rock	505	491	542	510
17	A_1	SiH_3 rock	515	526	581	550
18	B_2	SiH_2 rock	568	567	624	596
19	A_2	twist	646	647	711	674
20	B_1	wag	665	655	721	678
21	B_2	twist	705	703	773	736
22	A_2	wag	732	733	806	768
23	A_1	twist	740	742	816	770
24	B_1	wag	797	799	879	830
25	B_1	SiH_3 s-def	892	890	982	931
26	A_1	SiH_3 s-def	892	895	988	938
27	A_1	SiH_2 scissor	926	927	1019	972
28	B_1	SiH_2 scissor	929	929	1022	973
29	A_1	SiH_2 scissor	933	931	1024	978
30	A_2	SiH_3 def	939	937	1034	993
31	B_2	SiH_3 def	939	938	1034	993
32	B_1	SiH_3 def	941	941	1038	997
33	A_1	SiH_3 def	941	944	1041	999
34	B_2	SiH_2 stretch	2112	2117	2315	2285
35	A_2	SiH_2 stretch	2113	2119	2318	2287
36	B_1	SiH_2 stretch	2122	2120	2319	2290
37	A_1	SiH_2 stretch	2122	2121	2320	2294
38	B_2	SiH_2 stretch	2123	2125	2325	2299
39	A_1	SiH_2 stretch	2124	2128	2328	2304
40	B_1	SiH_3 stretch	2142	2141	2343	2305
41	A_1	SiH_3 stretch	2142	2142	2343	2306
42	B_1	SiH_3 stretch	2142	2142	2343	2319
43	A_1	SiH_3 stretch	2142	2143	2344	2319
44	A_2	SiH_3 stretch	2144	2144	2345	2319
45	B_2	SiH_3 stretch	2144	2146	2348	2320
error				4.0	0	116.7	92.8

[a] The MSXX column gives the predictions for the FF derived in this paper. [b] Scaled from HF using factors from Table 4.[11b] [c] 6-31G** basis. [d] The accordion mode.

the barriers between the local minimas are usually not available from experiment.

To circumvent this problem, we consistently use *ab initio* calculations to provide the torsional potential energy surface. With the 6-31G** basis, the torsional potentials calculated from HF wave functions are adequate.[12]

The HF calculations lead to a total torsional potential function $E^{HF}(\phi)$ which we want to fit with the FF,

$$E^{HF}(\phi) \cong E^{FF}(\phi) = E^{FF}_{notor}(\phi) + E^{tor}(\phi) \qquad (12)$$

where

$$E^{FF}_{notor}(\phi) = E^{val}_{B,A}(\phi) + E^{Q}(\phi) + E^{vdW}(\phi)$$

Here $E^{val}_{B,A}$ contains all parts of E^{val} *except* for the torsional term to be fitted. We have already specified how E^{Q} and E^{vdW} are to be calculated, and the dependence of $E^{val}_{B,A}$ on bonds and angles will be determined in section E. Thus we *define* the torsional potential as

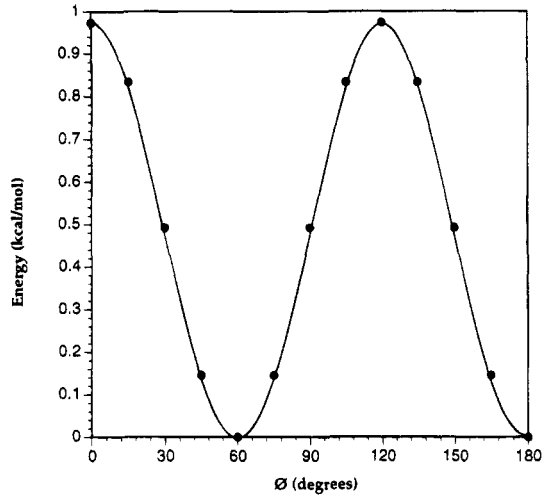

Figure 1. Torsional potential (kcal/mol) of Si_2H_6 from HF calculations and from the MSXX FF. All bonds and angles are optimized for each ϕ The total $E^{HF}(\phi)$ and $E^{FF}(\phi)$ is plotted. The HF energies are plotted as symbols.

$$E^{tor}(\phi) \equiv E^{HF}(\phi) - E^{FF}_{notor}(\phi) \qquad (13)$$

In determining $E^{tor}(\phi)$ from (13), the simplest procedure would be to determine the nonadiabatic surface by fixing all bonds and angles so that only the torsional angle ϕ changes. However, such rigid rotations about bonds sometimes lead to unfavorable contacts with very short distances between nonbonded atoms. In such cases the *ab initio* wave function readjusts the molecular orbitals to minimize these repulsions. However, the functional form of E^{vdW} is derived from fits to experimental data on equilibrium packings of molecules and may not accurately describe the inner repulsive wall. As a result such bad contacts can lead to very large values for $E^{FF}_{notor}(\phi)$ in (13). Consequently the adiabatic torsional potential is calculated by fixing ϕ and optimizing all other degrees of freedom at each conformation. For the HF wave function we optimize all other geometric parameters at each ϕ, and for $E^{FF}(\phi)$ we do the same. Then we solve (13) to obtain the torsional potential. Since the torsional constants are derived from these calculations of the torsional potential, we use zero weights on the torsional modes when using the Hessian biased procedure for the other valence interactions.

The HF wave function was calculated by fixing the dihedrals of interest (in increments of 15°) and optimizing all other degrees of freedom, leading to the results in Figures 1−3 and Table 3. For Si_3H_8 we calculated the 2-D surface where the two Si−Si dihedrals ϕ_1 and ϕ_2 are varied. Since the grid is sparse, a bicubic spline was fitted to generate a denser grid.

The FF uses a Fourier series of torsional terms

$$E^{tor}(\phi) = \sum_{m=0}^{12} K_m \cos m\phi \qquad (14)$$

For a given JK dihedral about a single bond, there are nine possible IJKL terms. Each torsional term is scaled by the number of torsions about the bond, nine in this case, so that the torsional barriers V_m represent the full torsional barrier about each bond.

Parts a−c of Table 3 show $E^{HF}(\phi)$ and $E^{FF}(\phi)$ for Si_2H_6 and $E^{HF}(\phi_1,\phi_2)$ and $E^{FF}(\phi_1,\phi_2)$ for Si_3H_8. The fit to the *ab initio* energy surface was Boltzmann weighted so that the errors near the minima are smaller than the errors near the maxima. [Since the higher barrier regions will be sampled less in molecular dynamics (MD), larger errors near the potential maxima can be

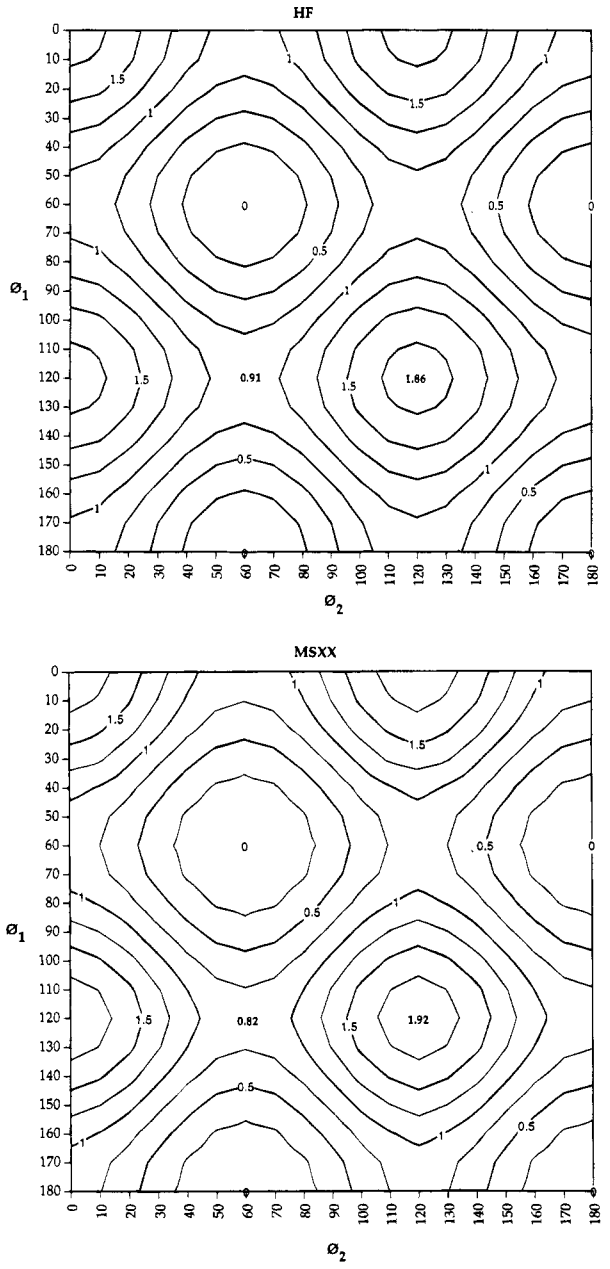

Figure 2. Torsional potential (kcal/mol) of Si_3H_8 from (a, top) HF calculations and (b, bottom) the MSXX FF. Each is plotted versus the two dihedral angles ϕ_1 = $HSiSi_2Si_3$ and ϕ_2 = $SiSi_2Si_3H$ (abscissa and ordinate, respectively). All other bonds and angles are optimized for each ϕ_1 and ϕ_2.

tolerated more easily than near the minima.] We found that a single V_3 barrier of 0.94 kcal/mol for HSiSiH was sufficient for Si_2H_6. For Si_3H_6, we kept the same HSiSiH term and found that for HSiSiSi a single V_3 term (barrier of 0.806 kcal/mol) was sufficient. For n-Si_4H_{10} we used the above values and described the SiSiSiSi interaction with three terms (V_1, V_2, and V_3). The resultant PES are plotted in Figures 1−3 for HF and MSXX.

II.F. Valence Force Field Terms. The bond and angle part of the valence FF is written as

$$E^{\text{val}}_{\text{B,A}} = E^{\text{bond}} + E^{\text{angle}} + E^{\text{cross}}$$

We take E^{bond} as a sum over all bond pairs, each of which has the form of a Morse function,[7]

$$E^{\text{Morse}}(R) = D_R[\chi - 1]^2 \tag{15a}$$

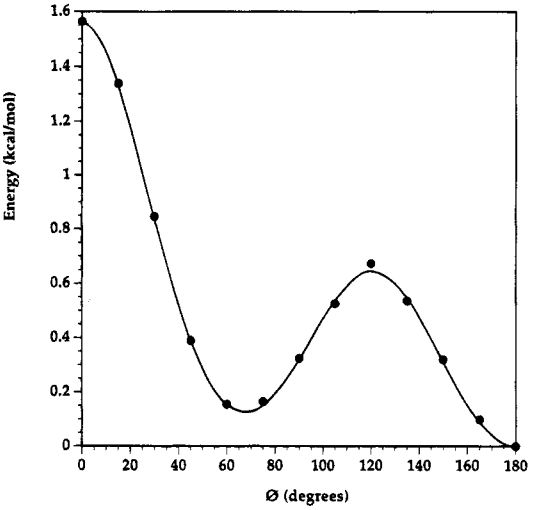

Figure 3. Torsional potential (kcal/mol) for the central SiSi bond of $H_3SiSiH_2SiH_2SiH_3$ from HF and HBFF. All other bonds and angles are optimized for each ϕ. The HF energies are plotted as symbols.

with

$$\chi = e^{-\alpha(R-R_e)} \tag{15b}$$

$$\alpha = [K_R/2D_R]^{1/2} \tag{15c}$$

This includes anharmonicity and allows bond dissociation. Here there are three independent parameters R_e, k_R, and D_R. Since D_R is not sensitive to the Hessian or geometry, we choose D_R based on the experimental bond energy (it was not optimized).

We take E^{angle} as a sum over all six angle terms IJK for each atom J, where each angle term is described with the cosine angle form,[7]

$$E^{\cos}(\theta) = \frac{C}{2}[\cos\theta - \cos\theta_e]^2 \tag{16a}$$

with

$$C = \frac{K_\theta}{\sin^2\theta_e} \tag{16b}$$

This form leads correctly to $dE/d\theta = 0$ for $\theta = 0$, 180° and has a barrier of

$$E^{\text{barrier}} = \frac{C}{2}[1 + \cos\theta_e]^2 \tag{17}$$

We found that bond−bond cross-terms

$$E_{\text{1BB}} = K_{RR'}(r_1 - r_1^e)(r_2 - r_2^e) \tag{18}$$

sharing an apex atom (e.g., IJ and JK for the atoms I and K bonded to J) are generally useful when the two are equivalent (e.g., SiH/SiH at SiH_3 or SiH_2 groups). However SiSi/SiH at the SiH_3 group does not have much effect on the FF. This is because the splitting between equivalent terms is dominated by off-diagonal interactions, whereas analogous couplings for inequivalent bonds can be built into the force field by modifying the diagonal terms. Thus, we include bond−bond cross terms only for equivalent bonds.

TABLE 6: Vibrational Frequencies (cm^{-1}) for SiH_4

mode	sym	HBFF	exptl[a]	HF[b]	MP2[b]	MSXX	scale exptl/HF	exptl[a] SiD_4	MSXX SiD_4
1	T_2	914.0	914.0	1017.1	973.7	883.1	0.899	674	669.9
2	E	975.0	975.0	1053.4	1017.6	970.7	0.926	685	689.5
3	A_1	2187.0	2187.0	2370.0	2339.3	2151.6	0.923	1563	1546.4
4	T_2	2191.0	2191.0	2360.6	2349.9	2154.2	0.928	1598	1585.8
rms error		0.0		140.6	116.0	25.5			10.7

[a] Reference 15. [b] 6-31G** basis.

Bond−angle cross-terms (e.g., bond IJ with angle IJK),

$$E_{1BA} = D_{R\theta}(r_1 - r_1^e)(\cos\theta_1 - \cos\theta_1^e) \quad (19)$$

are necessary for a good description of the vibrations. For a given IJK there are two such terms, one for r_{IJ} and one for r_{JK}.

In addition we find that one-center angle−angle cross-terms (involving bonds defining two angles sharing a common bond and the apex atom) are important,

$$E_{1AA} = F_{\theta\theta}(\cos\theta_1 - \cos\theta_1^e)(\cos\theta_2 - \cos\theta_2^e) \quad (20)$$

The sign and magnitude of these terms are difficult to predict *a priori*. Hence, we started with various combinations of sign and magnitude and allowed the optimization to determine these coupling constants.

For long-chain molecules, we found that two-center angle−angle cross-terms are also important,

$$E_{2AA} = G_{\theta\theta}(\cos\theta_1 - \cos\theta_1^e)(\cos\theta_2 - \cos\theta_2^e)f(\phi) \quad (21)$$

Thus, for the dihedral IJKL, θ_1 corresponds to the IJK angle and θ_2 corresponds to JKL. For disilane such terms determine the splitting between rocking modes of different symmetries. In the case of polyethylene,[11a] they are essential in reproducing the stiffness in the chain direction. For zinc blende and diamond solids (e.g., diamond, silicon, GaAs, etc.) they are necessary for describing the mode softening of the transverse acoustic (TA) mode near the zone boundary.[13] In P(SiH), we find that they are important for predicting the modulus in the chain direction. Since only cis and trans coupling are important in P(SiH) so that $f(0°) = f(180°) = 1$ and $f(60°) = f(300°) = 0$, and we want the function to smoothly vary with ϕ, the factor $f(\phi)$ is chosen as

$$f(\phi) = {}^1/_3[1 - 2\cos\phi]$$

Summarizing we take

$$E^{cross} = \sum E_{1BB} + \sum E_{1BA} + \sum E_{1AA} + \sum E_{2AA} \quad (22)$$

II.G. Optimization of Parameters. We used the program FFOPT[14] developed by Dasgupta, Yamasaki, and Goddard to optimize the valence HBFF parameters. This uses singular value decomposition (SVD) and emphasizes changes in parameters that most affect the properties of interest (and eliminates parameter redundancies).

III. Polysilane Oligomers

III.A. SiH_4. The vibrational frequencies for silane are shown in Table 6, and the silane FF is shown in Table 7a. HBFF exactly reproduces the geometry and the experimental frequencies.[15] MSXX (based on n-Si_4H_{10}) leads to slightly low (about 1%) frequencies for silane, and the inaccuracy in applying the MSXX to disilane and trisilane is much smaller. (Table 6 also shows the accuracy of the silane HBFF for predicting the frequencies of deuterated silane.[15]) This indicates the robustness of the MSXX.

The MSXX FF parameters to be used for all P(SiH) oligomers are shown in Table 7a (the calculated oligomer geometries are in Table 1). The MSXX FF leads to excellent geometries and frequencies.

III.B. Si_2H_6. Disilane is the largest oligomer of P(SiH), having a complete set of experimental vibrational assignments.[16] In addition, all the isotopic shifts, except for the torsional mode, are available for fully deuterated disilane. Table 8 shows predicted frequencies, where we find an rms difference of 4.8 cm^{-1} between HBFF and experiment.[16] The HBFF accurately reproduces the geometry as shown in Table 1. The validity of the FF is shown by its accurate prediction of the Si_2D_6 experimental frequencies[17] as shown in Table 8. Our FF includes only a limited set of cross-terms. As a result there will be small rms errors in the frequencies for all molecules except the smallest. For example, in Si_2H_6, the couplings of the Si−Si torsion with all other coordinates is ignored in fitting the FF.

The experimental frequencies for disilane include the torsional mode (determined indirectly from a two photon process); however, we do not use this in our fit. As discussed above, the torsional potential is fitted to the entire torsional potential surface. Disilane is the only P(SiH) oligomer for which we can compare the torsional frequency for the single bond rotational potential to experimental data. Figure 1 and Table 3a show the accurate match of the *ab initio* and HBFF torsional potentials over the entire dihedral angle range. This accuracy comes at the modest cost of an error of 8.2 cm^{-1} in the torsional frequency.

III.C. Si_3H_8. Silylpropane is the smallest model compound containing the $[-SiH_2-]$ repeating unit of P(SiH). Some experimental data (13 of 27 modes)[18] are available on the vibrational frequencies of Si_3H_8, but a complete set of experimental frequencies for the isolated molecule in the gas phase is not available. Consequently, for each class we considered only the experimentally known vibrations to obtain the accurate scale factor for that class, which was then applied to all *ab initio* frequencies to predict the complete set of "experimental" frequencies. Using these scales from within the same molecule leads to very small standard deviations of the scales and thus is likely to yield accurate scaling of the experimentally unassigned modes. The average error between the HBFF frequencies and the experimentally available frequencies[18] is 7.7 cm^{-1} (6.0 cm^{-1} including the scaled HF frequencies). Table 9 also shows the frequencies for two deuterated species to compare with future experimental results.

We find that fitting the FF to experiment requires the use of different valence terms for the SiH_2 hydrogens and the SiH_3 hydrogens (we use the HSiSiH torsional potential transferred from disilane). Using the MSXX FF from n-Si_4H_{10} to calculate the modes of Si_3H_8 leads to good accuracy, especially for the geometry (Table 1). This justifies the transferability of the parameters between molecules and indicates that the MSXX FF should be accurate for describing P(SiH) and other oligomers.

TABLE 7

(a) Parameters for the MSXX FF of Various Polysilane Oligomers

valence terms		SiH_4	Si_2H_6	Si_3H_8[a]	n-Si_4H_{10}[a]	n-Si_5H_{12}
				Bonds (See Equation 15)		
SiH	K_R	396.3	399.8	399.4 (381.8)	395.8 (383.1)	377.7 (385.7)
	R_e	1.476	1.471	1.468 (1.477)	1.468 (1.476)	1.479 (1.474)
	D_R[b]	92.6	92.6	92.6	92.6	92.6
SiSi	K_R		276.7	256.7	278.8 (261.1)	267.9 (253.5)
	R_e		2.369	2.344	2.330 (2.328)	2.321 (2.363)
	D_R[b]	73.7	73.7	73.7	73.7	73.7
				Angles (See Equations 16−20)		
HSiH	K_θ	68.35	55.96	50.91 (64.90)	56.39 (56.05)	50.4 (59.2)
	θ_e	110.4	113.1	117.2 (109.46)	113.6 (113.4)	118.1 (111.6)
	$D_{R\theta}$	−1.90	−10.16	−9.17 (−5.91)	−11.2 (−1.46)	2.49 (−12.0)
	$K_{RR'}$	4.30	2.39	4.05 (4.20)	3.34 (4.46)	4.43 (3.51)
SiSiH	K_θ		42.25	39.30 (43.02)	45.0 (33.3, 41.6)	35.4 (43.1, 42.2)
	θ_e		115.14	120.78 (110.62)	117.2 (118.5, 115.8)	123.3 (114.4, 114.0)
	$D_{R\theta}$ (SiSi)		16.14	−8.57 (−2.69)	−5.34 (−6.41, −4.16)	−6.05 (−5.67, 5.74)
	$D_{R'\theta}$ (SiH)		−10.67	−9.23 (−7.02)	−10.54 (−10.64, −2.68)	−2.04 (−7.47, −13.94)
SiSiSi	K_θ			42.53	35.4	26.1 (75.9)
	θ_e			122.55	126.6	126.0 (114.6)
	$D_{R\theta}$			−6.19	−15.6 (−18.7)	−22.9, (−11.1 −18.6)
	$K_{RR'}$			15.21	0.635	0.515 (0.518)
				Torsions (See Equations 14 and 21)		
SiSiSiSi	K_1				5.86	4.60
	K_2				3.54	6.32
	K_3				0.46	−1.02
	$F_{\theta\theta}$				−9.28	−13.2
HSiSiSi	K_3			0.806	0.806 (0.806)	0.806 (0.806)
	$F_{\theta\theta'}$			−2.33	−7.93 (−9.36)	−7.35 (−9.95)
HSiSiH	K_3		0.940	0.940	0.940 (0.940)	0.940 (0.940)
	$F_{\theta\theta}$		−14.749	−15.062	−13.401 (−13.401)	−15.468 (−15.288)
				One-Center Angle−Angle (See Equation 20)		
SiSiHH	$G_{\theta\theta}$		−0.178	0.086 (−1.203)	−0.67 (−0.46, −0.51)	−0.55 (−0.57)
SiSiSiH	$G_{\theta\theta'}$		−0.673	−1.51	−1.621 (−1.583)	−1.32
SiHSiH	$G_{\theta\theta'}$		−0.333	−1.413 (0.311)	−1.108 (−1.184, −2.204)	−1.56
SiHSiSi	$G_{\theta\theta}$		−1.259	−3.900		−4.775
SiHHH	$G_{\theta\theta}$	5.717		−0.233	−0.349	0.328

(b) MSXX FF for Polysilane Polymers[b]

bonds	R_e	K_R	D_R	bonds	R_e	K_R	D_R	bonds	R_e	K_R	D_R
H−Si_4	1.476	396.3	92.6	H−Si_2	1.476	383.1	92.6	Si_3−Si_2	2.330	278.8	73.7
H−Si_3	1.478	395.8	92.6	Si_3−Si_3	2.369	276.7	73.7	Si_2−Si_2	2.328	261.1	73.7

angles	θ_e	K_θ	$K_{RR'}$	$D_{R\theta}$	$D_{R'\theta}$	angles	θ_e	K_θ	$K_{RR'}$	$D_{R\theta}$	$D_{R'\theta}$
H−Si_4−H	110.4	68.35	4.30	−1.90	−1.90	Si_3−Si_2−H	118.5	33.3		−6.41	−10.64
H−Si_3−H	113.6	56.39	3.34	−11.20	−11.20	Si_2−Si_2−H	115.8	41.6		−4.16	−2.68
H−Si_2−H	113.4	56.05	4.46	−1.46	−1.46	Si_3−Si_2−Si_3	122.55	42.53	15.21	−6.19	−6.19
Si_3−Si_3−H	115.14	42.25		16.14	−10.67	Si_2−Si_2−Si_3	126.6	35.4	0.635	−15.6	−18.7
Si_2−Si_3−H	117.2	45.0		−5.34	−10.54	Si_2−Si_2−Si_2					

torsions	K_0	K_1	K_2	K_3	$F_{\theta\theta}$
H−Si−Si−H	0.940			0.940	−13.4
H−Si−Si−Si	0.806			0.806	−9.36
Si−Si−Si−Si	2.785	5.86	3.54	0.46	−9.28

one-center angle−angle	$F_{\theta\theta}$	one-center angle−angle	$F_{\theta\theta}$
Si_4−H−H−H	5.717	Si_2−Si−H−H	−4.775
Si_3−H−H−H	−0.349	Si_2−Si−Si−H	−1.6
Si_3−Si−H−H	−1.108		

(c) van der Waals Parameters[7] Used for All MSXX Force Fields, $E_{vdw} = D_v(\varrho^{-12} - 2\varrho^{-6})$, Where $\varrho = R/R_v$[c]

vdW parameters	Si	H	vdW parameters	Si	H
R_v (Å)	4.270	3.195	D_v (kcal/mol)	0.310	0.0152

[a] Values in parentheses refer to terms involving the central hydrogens. [b] Not optimized. [c] The off-diagonal parameters D_v and R_v (Si−H) are obtained from the diagonal parameters by using the geometric mean.

The torsional modes were not obtained from HBFF. In the Si_3H_8 FF we use the HSiSiH torsional potential from disilane and fit a Fourier series (14) to describe the torsional potential energy surface for the two HSiSiSi dihedrals. Figure 2 and Table 3b show the accuracy of the HBFF.

III.D. n-Si_4H_{10}. n-Si_4H_{10} is the smallest oligomer which

TABLE 8: Vibrational Frequencies (cm^{-1}) for Si_2H_6

mode	sym	character	HF[a]	scale[g]	MP2	exptl[b]	HBFF Si_2H_6	Cui *et al.*[c]	MSXX	HBFF[f] Si_2D_6	expt[d] Si_2D_6
1	A_{1u}	torsion	134.3	0.931	143.6	125.0	133.2		133.3	94.2	
2	E_u	SiH_3 rock	416.6	0.910	385.7	379.3	379.7	400	377.9	271.3	277.0
3	A_{1g}	SiSi str	464.0	0.936	458.9	434.2	435.2	418	418.9	379.2	407.5
4	E_g	SiH_3 rock	697.1	0.897	666.8	625.2	625.2	644	630.9	475.4	474.7
5	A_{2u}	SiH_3 def	947.9	0.890	900.5	843.5	844.9	856	870.1	622.1	624.9
6	A_{1g}	SiH_3 def	1031.5	0.881	980.1	909.0	907.0	922	872.9	730.7	683.1
7	E_u	SiH_3 def	1043.1	0.891	984.7	929.3	931.5	964	939.9	668.6	667.0
8	E_g	SiH_3 def	1027.5	0.914	1001.3	939.6	937.1	952	942.4	668.9	682.9
9	A_{2u}	SiH_3 str	2337.1	0.880	2309.7	2145.3	2152.4	2145	2137.5	1531.0	1549.3
10	A_{1g}	SiH_3 str	2352.7	0.915	2319.5	2152.0	2154.9	2160	2139.7	1534.8	1547.5
11	E_g	SiH_3 str	2337.3	0.922	2323.3	2155.6	2166.2	2154	2137.4	1564.1	1569.0
12	E_u	SiH_3 str	2346.7	0.928	2331.7	2178.6	2168.2	2164	2139.0	1566.0	1585.0
rms[e]			126.6		101.5		4.8	16.5	14	19.5	

[a] 6-31G** basis. [b] Reference 16. [c] Reference 5. [d] Reference 17. [e] Excluding the torsional frequency, a_{1u}, which was not fit. [f] Using the HBFF for Si_2H_6. [g] ν_{expt}/ν_{HF}.

TABLE 9: Vibrational Frequencies (cm^{-1}) for Si_3H_8

mode	sym	character	HF[e]	scale	MP2[e]	expt[a]	HBFF	Cui FF *et al.*[5]	MSXX	HBFF Si_3D_8	HBFF $Si_3D_2H_6$
1	A_2	torsion	77.3		107.6	[72]	89.1		88.7	63.4	89.1
2	B_2	torsion	99.2		108.0	[92]	94.7		95.2	69.9	94.3
3	A_1	SiSiSi bend[c]	109.3	1.025	120.0	112[b]	113.4	107	109.9	103.9	112.6
4	B_2	SiH_2 rock	353.0		291.9	[317]	321.4	337	324.6	232.3	253.7
5	A_1	SiSi	411.3	0.953	395.8	392[b]	394.1	371	375.9	303.1	387.9
6	A_2	twist	464.1		430.9	(420)	422.8	476	421.2	344.1	357.5
7	B_1	SiSi	485.3	0.921	458.5	447[b]	447.9	445	447.2	354.2	389.9
8	B_1	wag	502.1	0.932	477.2	468[b]	476.1	446	470.7	400.5	460.6
9	A_1	SiH_3 rock	625.0	0.904	596.4	565[b]	545.6	582	539.0	430.7	544.9
10	B_2	SiH_3 rock	657.4	0.888	624.5	584[b]	600.0	606	603.0	465.1	577.4
11	A_2	SiH_2 twist	777.8	0.905	730.1	704[b]	703.5	733	693.4	510.7	591.8
12	B_1	SiH_2 wag	810.7	0.883	751.9	716[b]	714.7	740	748.9	567.5	612.9
13	B_1	SiH_3 s-def	983.0	0.891	931.8	876[b]	883.6	881	859.2	658.5	883.6
14	A_1	SiH_3 s-def	989.9		939.2	(895)	887.2	897	862.3	657.9	672.1
15	A_1	SiH_2 scissor	1025.9	0.903	973.5	926[b]	929.1	940	927.2	674.3	887.2
16	A_2	SiH_3 d-def	1032.3		991.9	(933)	935.9	954	939.5	670.5	935.6
17	B_2	SiH_3 d-def	1036.2		993.6	(937)	936.2	959	939.9	670.9	936.1
18	B_1	SiH_3 d-def	1034.6		995.6	(935)	937.7	959	940.9	671.8	937.6
19	A_1	SiH_3 d-def	1044.8		1001.4	(944)	940.1	965	943.1	672.7	939.8
20	B_2	SiH_2 str	2321.3		2302.3	(2128)	2127.8	2145	2127.3	1537.4	1537.2
21	A_1	SiH_3 str	2320.0	0.918	2305.9	2130[b]	2130.3	2137	2128.3	1524.6	1525.2
22	A_2	SiH_3 str	2338.3		2315.4	(2143)	2145.5	2149	2144.5	1549.6	2145.5
23	B_1	SiH_3 str	2339.7		2317.7	(2144)	2145.8	2156	2144.3	1527.7	2145.8
24	B_2	SiH_3 str	2345.0	0.916	2318.9	2148[b]	2146.2	2158	2145.3	1550.1	2146.1
25	A_1	SiH_3 str	2344.4		2319.7	(2149)	2146.6	2159	2145.3	1529.1	2146.6
26	B_1	SiH_3 str	2343.5		2340.7	(2148)	2149.2	2163	2146.6	1551.5	2149.1
27	A_1	SiH_3 str	2350.1	0.915	2352.7	2150[b]	2149.6	2164	2147.1	1551.9	2149.5
rms			122.5		102.9		6.0[d] (7.7)	17	12.65		

[a] The values in parentheses and brackets are not available from experiment and were scaled from HF. The values in parentheses used scaling from corresponding modes of Si_3H_6; the values in brackets (torsions) used the scale for Si_2H_6. [b] Reference 18. [c] Accordion mode. [d] Excluding the two torsional frequencies fit using the full PES. [e] 6-31G** basis.

includes all the valence terms necessary to model larger oligomers and P(SiH). This is the basis for the MSXX FF to be used for P(SiH). Thus, MSXX uses the valence terms describing the central silicons of *n*-Si_4H_{10} to describe the larger oligomers and the polysilane crystals. The *n*-silylbutane HBFF not only includes all the terms to simulate the smallest oligomers, it also includes all the terms necessary to model the larger oligomers and P(SiH) and thus can be used to predict the properties of P(SiH) of arbitrary chain length.

Only a partial assignment from experimental spectra[18] is available, and we follow the same procedure used for scaling of the silylpropane frequencies. Table 10 shows the HF frequencies, the experimental assigned frequencies, and the scales used for modes not observed. The narrow range in scaling factors for similar modes indicates the validity of this procedure. The HBFF procedure reproduces the experimental frequencies and scaled HF frequencies to 6.2-cm^{-1} rms error. The geometry is accurately reproduced as shown in Table 1.

For *n*-Si_4H_{10} we also develop the MSXX-R FF which does not distinguish between SiH_3 and SiH_2. We find that MSXX-R is only slightly worse than the MSXX, as shown in Table 10.

The torsional mode was not scaled but was calculated by fitting a Fourier series (14) to the rotations of the molecule about the SiSiSiSi dihedral. The HSiSiSi and HSiSiH torsional potentials were transferred from silylpropane and disilane, respectively, and not varied. Figure 3 and Table 3c show the HBFF and the *ab initio* torsional potential.

III.E. *n*-Si_5H_{12}. The *n*-Si_5H_{12} molecule has not been observed experimentally. We calculated vibrational frequencies using both the HF/6-31G** and MP2/6-31G** methods to obtain validation of the MSXX FF (from Si_4H_{10}). Scales from the smaller oligomers are applied to the *n*-Si_5H_{12} HF vibrational frequencies to obtain scaled HF frequencies which can be compared to frequencies calculated using the MSXX. Table 5 compares the MSXX frequencies and the scaled HF frequencies. The rms difference is less than 12 cm^{-1}, with most modes

TABLE 10: Vibrational Frequencies (cm^{-1}) for *n*-Butylsilane, *n*-Si_4H_{10}[a]

mode	sym	character	MSXX-R	MSXX	expt	Cui et al.[g]	HF[f]	scale	MP2
1	Au	SiSi torsion	23.6	32.1	24.8[b]		24.8		47.5
2	Bu	SiSiSi bend	73.1	73.8	73.2[b]		73.2		77.2
3	Au	SiH_3 torsion	97.6	92.5	80.3[c]		86.3		110.0
4	Bg	SiH_3 torsion	102.7	97.8	88.0[c]		94.6		115.5
5	Ag	SiSiSi bend[h]	141.7	131.5	139[c]	130	132.8	1.047	126.2
6	Au	SiH_2 rock	307.6	307.8	306.4	320	337.0		310.9
7	Bg	twist−rock	355.5	350.2	349.4[c]	368	384.3		362.0
8	Ag	SiSi stretch	357.1	358.7	361[c]	357	394.6	0.915	379.6
9	Bu	SiSi stretch	420.5	422.0	422[d]	418	461.5	0.914	442.8
10	Au	twist−rock	453.0	465.7	465[d]	474	492.3	0.945	468.2
11	Ag	SiSi stretch	462.6	470.7	465[d]	459	503.3	0.924	484.6
12	Bu	wag	492.4	493.1	478[d]	498	525.8	0.909	495.3
13	Ag	SiH_3 rock	527.5	527.8	542[d]	556	595.9	0.910	566.3
14	Bg	SiH_2 rock	581.6	577.8	577.0[c]	587	636.5		608.9
15	Au	twist	668.7	651.1	657[d]	693	739.4	0.889	705.7
16	Bu	wag	718.9	709.4	692[d]	694	754.7	0.917	709.7
17	Bg	twist	721.0	743.8	744[d]	753	798.7	0.932	761.5
18	Ag	wag	782.5	782.1	784.1[d]	780	862.5		815.6
19	Bu	SiH_3 s-def	865.6	871.4	874[d]	883	981.1	0.891	931.4
20	Ag	SiH_3 s-def	868.4	874.1	869[d]	891	988.9	0.879	939.4
21	Ag	SiH_2 scissor	924.1	924.9	917[d]	941	1024.0	0.896	975.1
22	Bu	SiH_2 scissor	924.4	927.3	933[d]	943	1021.8	0.913	975.8
23	Bg	SiH_3 d-def	940.5	939.8	937.6[c]	956	1034.1		993.5
24	Au	SiH_3 d-def	941.2	940.5	938.0[c]	957	1034.7		993.7
25	Bu	SiH_3 d-def	941.7	941.5	941.7[c]	963	1040.6		997.1
26	Ag	SiH_3 d-def	942.4	942.2	943.4[c]	961	1038.7		998.6
27	Bg	SiH_2 str	2123.7	2120.5	2119.5[c]	2142	2316.8		2286.4
28	Au	SiH_2 str	2125.2	2121.0	2125.7[c]	2148	2317.6		2287.5
29	Bu	SiH_2 str	2125.8	2121.6	2120.6[c]	2136	2318.0		2295.2
30	Ag	SiH_2 str	2126.4	2123.5	2120[d]	2139	2321.5	0.913	2301.6
31	Bg	SiH_3 str	2139.3	2141.7	2143[d]	2159	2341.8	0.915	2303.8
32	Ag	SiH_3 str	2139.5	2141.9	2144[d]	2158	2345.0	0.914	2306.8
33	Bu	SiH_3 str	2139.5	2143.4	2143.6[c]	2154	2343.2		2318.3
34	Ag	SiH_3 str	2139.7	2144.8	2142.9[c]	2158	2342.4		2320.4
35	Bu	SiH_3 str	2140.9	2143.6	2144.1[c]	2161	2343.8		2319.6
36	Ag	SiH_3 str	2148.2	2151.5	2148.5[c]	2160	2348.5		2319.0
rms			7.3 (7.1)	6.2 (6.0)	0.0	16[e]	119.4		95.3

[a] Experiment (expt) includes the best estimate of the experiment using scaled HF results. The MSXX force field distinguishes between the SiH_2 and SiH_3 centers. The MSXX-R FF does *not* distinguish. [b] *Ab initio* frequencies. [c] *Ab initio* frequencies scaled by *n*-Si_4H_{10} frequencies. [d] Reference 16. [e] Excluding the torsional frequencies (not fitted). [f] 6-31G** basis. [g] Reference 5. [h] The accordion mode.

TABLE 11: Predicted Structure of *n*-Si_5H_{12}[a]

	MSXX	HF[b]	Δ
Si_c-Si_{cc}	2.365	2.361	0.004
Si_c-Si	2.355	2.357	0.002
H_c-Si_c	1.480	1.482	0.002
$H_{cc}-Si_{cc}$	1.479	1.482	0.003
$H_{ip}-Si$	1.478	1.479	0.001
$H_{op}-Si$	1.478	1.479	0.001
$Si-Si_c-Si_{cc}$	112.1	112.69	0.59
$Si_c-Si_{cc}-Si_c$	114.16	113.03	1.13
$H_{ip}-Si-Si_c$	110.06	110.63	0.57
$H_{op}-Si-Si_c$	110.04	110.14	0.10
$H_{cc}-Si_{cc}-H_{cc}$	106.63	107.25	0.62
$H_c-Si_c-Si_{cc}$	110.06	108.93	1.13
$H_{op}-Si-Si_c-Si_{cc}$	59.95	59.81	0.14

[a] Distances are in angstroms; angles are in degrees. [b] 6-31G** basis.

differing less than 2%. Either method provides an acceptable prediction of experimental frequencies; however, MSXX requires substantially less computational time. MP2 *ab initio* calculations take substantially more time than scaled HF calculations but still overestimate experiment by 3−8% (Table 5), with the exception of the low energy skeletal modes. Since scaled HF and MSXX predictions are generally within 1% of the experimental frequencies, we conclude that MSXX is the most cost-effective approach to predicting experimental frequencies. Table 11 compares the geometries for *n*-Si_5H_{12} from HF and from the MSXX. The differences are small, with the largest error (1.1°) for the SiSiSi central angle.

IV. Polysilane

We base the MSXX FF for polysilane polymers on the parameters for the central atoms of the HBFF for *n*-Si_4H_{10} in Table 7a. We refer to this as the MSXX FF (see Table 7b). The charges for polysilane polymer were based on the PDQ atomic charges for the central SiH_2 group of *n*-Si_5H_{12} (see Table 2).

Particularly important for calculations on P(SiH) polymers are the SiSiSi bends denoted as accordion modes in Tables 5, 9, and 10. This mode is prominent in the Raman spectra for long alkanes, and extrapolating the frequency of this mode to infinite alkanes leads to an excellent prediction of the Young's modulus (see ref 11a for discussion).

The MSXX FF was used to calculate the properties of the crystal built with the all-trans conformation of P(SiH). This is analogous to polyethylene (PE) except that structures with both one and two chains per cell were considered. Table 12 shows the structure and mechanical properties of the crystal at 0, 77, and 300 K.

The bulk modulus at 0 K is 13.10 GPa. The Young's moduli calculated are 11.94, 110.57, and 18.64 GPa at 0 K which compare to 9.0, 337.0, and 9.4 for PE at 0 K. PE is much stiffer along the chain direction than P(SiH). However, the Young's modulus perpendicular to the chains is softer for PE at low temperatures and similar in stiffness to P(SiH) at temperatures above 300 K. Because of the anharmonicity of vdW and electrostatic interactions between chains, the Young's moduli perpendicular to the chain direction decrease dramatically with

TABLE 12: Properties of P(SiH) at 0, 77, and 300 K from Gibbs Dynamics for a 2 × 4 × 4 Supercell (Containing 384 Atoms)

property	0 K	77 K	300 K
unit cell (Å)[a]			
a	8.422	8.526	8.833
b	3.966	3.9769	3.955
c	4.685	4.733	4.929
bulk modulus (GPa)			
B	13.095	10.412	4.594
Young's moduli (GPa)			
E_a	11.94	9.586	4.720
E_b	110.57	107.64	98.384
E_c	18.64	14.750	5.789
elastic constants (GPa)			
C_{11}	15.60	12.424	5.937
C_{22}	121.30	116.501	102.85
C_{33}	22.97	18.172	7.088
C_{12}	12.73	10.335	5.045
C_{13}	8.17	6.486	2.765
C_{23}	9.24	7.374	3.369
C_{44}	16.23	13.995	8.322
C_{55}	7.34	5.936	2.876
C_{66}	19.30	16.299	8.906

[a] Structure was constrained to remain orthorhombic during the dynamics.

TABLE 13: Predicted Cohesive Energy (kcal/(mol of SiH_2)) for Polysilane Crystal[a]

	total energy at min	zero-point energy[b]	lattice enthalpy at 0 K
isolated chain	3.224	8.568	11.792
crystal (2 chains)	−1.055	9.031	7.976
cohesive energy (2 chains)	4.279	−0.463	3.816
crystal (1 chain)	−1.231	9.053	7.822
cohesive energy (1 chain)	4.455	−0.485	3.970

[a] The cohesive energy at 0 K of 3.82 kcal/(mol of SiH_2) compares with 1.87 kcal/(mol of CH_2) for polyethylene crystal. [b] Using 5 × 5 × 5 points in the Brillouin zone.

temperature (by ≈65% for 0−300 K). The decrease in the Young's moduli of polyethylene is much smaller (≈35% for 0−300 K).

The elastic constants of P(SiH) behave similarly to those of polyethylene. Thus, C_{22}, the elastic constant along the chain direction, decreases by only 15% from 0 to 300 K. In PE the decrease is 5.9%. C_{11} and C_{33} for deformations perpendicular to the chain direction show a decrease of 65% while in PE the decrease is ≈40%. The relative decrease in the deformation properties with temperature is large relative to polyethylene (see Table 12), both along the chain direction and perpendicular to it, indicating that both the valence and nonbond interactions are more anharmonic for P(SiH) than for PE.

The properties at 77 and 300 K were calculated by averaging the crystal structures from the last 20 ps of a 30-ps Gibbs molecular dynamics calculation (Nosè plus Rahman−Parrinello[19]) at several temperatures to calculate the thermal expansion tensor. Using the thermal expansion tensor, we calculated the lattice parameters at the desired temperatures and calculated the properties of the crystal at that desired temperature (after reoptimizing the atomic positions for the new lattice constants).

The cohesive energy of the crystal is calculated to be 3.816 kcal/(mol of SiH_2) (Table 13). This compares with 1.8701 kcal/(mol of CH_2) for polyethylene calculated by Karasawa et al.[11a] also using the MSXX FF obtained with the biased Hessian approach. Their results compare favorably to experiment where the cohesive energy is measured to be 1.84 kcal/(mol of CH_2). The larger elastic constants perpendicular to the chain direction of P(SiH) compared to PE reflect the relatively stronger nonbonded interactions and larger cohesive energy.

TABLE 14: Vibrational Frequencies (cm^{-1}) for Polysilane Crystal P(SiH) with Two Chains per Unit Cell[a]

		polarization direction		
mode	description	[010]	[100]	[001]
1	interchain	63.6	63.6	63.6
2	interchain	95.7	95.7	96.3
3	interchain	98.1	98.1	98.1
4	skeletal torsion	152.2	152.2	152.2
5	skeletal torsion	160.9	160.9	160.9
6	SiH_2 rock	320.9	320.9	343.8
7	SiH_2 rock	357.7	348.9	348.9
8	SiSiSi bend	398.7	398.7	398.7
9	SiSiSi bend	403.2	403.2	403.2
10	SiSi stretch	509.5	509.5	509.5
11	SiSi stretch	532.3	532.3	532.3
12	SiH_2 rock	573.5	573.5	573.5
13	SiH_2 twist	573.5	573.5	573.5
14	SiH_2 rock	583.7	583.7	583.7
15	SiH_2 twist	648.5	649.0	648.5
16	SiH_2 wag	702.1	742.5	702.1
17	SiH_2 wag	771.7	771.7	771.7
18	SiH_2 twist	840.6	840.6	840.6
19	SiH_2 wag	871.5	871.5	871.5
20	SiH_2 twist	927.5	927.5	927.5
21	SiH_2 scissor	948.2	948.2	953.8
22	SiH_2 scissor	950.6	950.6	950.6
23	SiH_2 wag	954.5	940.1	940.1
24	SiH_2 scissor	954.7	954.7	954.7
25	SiH_2 scissor	964.7	964.7	964.7
26	SiH stretch	2150.2	2150.2	2150.2
27	SiH stretch	2151.8	2151.6	2151.6
28	SiH stretch	2152.2	2151.8	2153.9
29	SiH stretch	2153.1	2153.1	2153.1
30	SiH stretch	2154.5	2154.5	2160.1
31	SiH stretch	2155.3	2155.3	2155.3
32	SiH stretch	2161.3	2161.3	2161.3
33	SiH stretch	2164.3	2159.0	2159.0

[a] Only the values for k = (Γ point) are shown. The chain direction is [010].

TABLE 15: Vibrational Frequencies (cm^{-1}) of P(SiH)[a]

			isolated chain		crystal	
mode	sym	description	Cui *et al.*[b]	MSXX	MSXX	expt
1	Au	SiH_2 rock	311	307.7	367.9	
2	Ag	SiSiSi bend	413	396.8	407.2	
3	Ag	SiSi stretch	469	493.1	526.7	480
4	Au	SiH_2 twist	549	556.8	613.0	
5	Bg	SiH_2 rock	532	562.5	585.1	
6	Bu	SiH_2 wag	604	685.0	692.9	
7	Bg	SiH_2 twist	769	795.2	842.4	
8	Ag	SiH_2 wag	808	852.1	929.8	
9	Ag	scissor	943	936.4	949.4	909
10	Bu	scissor	953	935.6	974.7	905
11	Bg	SiH stretch	2140	2128.3	2146.6	2155
12	Bu	SiH stretch	2139	2128.5	2151.0	2100
13	Au	SiH stretch	2158	2132.6	2153.6	2100
14	Ag	SiH stretch	2150	2130.3	2156.5	2115

[a] The first two columns are for a single infinite chain, while last two columns are for the crystal with one chain per unit cell. [b] Reference 5.

Tables 14 and 15 show the vibrational frequencies for the crystal and for the infinite single chain, respectively. Calculations by Cui et al.[5] on single unpacked chains (ignoring vdW and Coulomb) are within 5−30 cm^{-1} of our results. Our results show that the inclusion of Coulombic and vdW forces in the MSXX FF strongly affects interactions between neighboring chains, as shown by the changes in the predicted vibrational frequencies between the packed and unpacked P(SiH). Our single chain frequencies are in better agreement with many of

TABLE 16: Packing of P(SiH) and Polyethylene[a]

lattice constant	P(SiH)	PE
unit cell		
a	8.422	7.121
b (chain)	3.966	2.546
c	4.685	4.851
a/$\bar{R}$	5.69	6.50
b/$\bar{R}$	1.69	1.64
c/$\bar{R}$	3.17	4.43

[a] R is the C−H (1.096 Å) or Si−H (1.48 Å) bond distance and $\bar{R}$ is the C−C (1.553 Å) or Si−Si (2.35 Å) bond distance for PE and P(SiH), respectively.

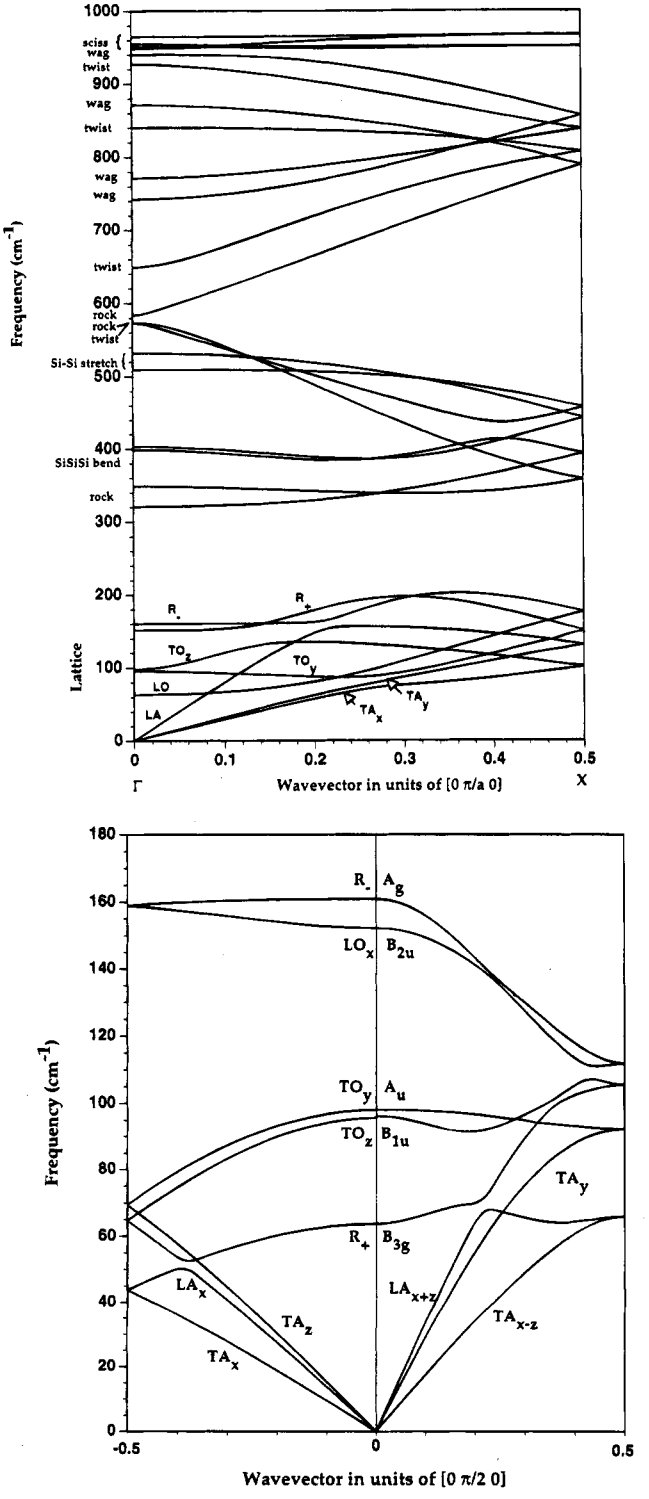

Figure 4. Calculated phonon modes (cm^{-1}) of crystalline P(SiH) for the (a, top) [010] and (b, bottom) [001] directions (the chain direction is [010]). Only the modes below 1000 cm^{-1} are shown.

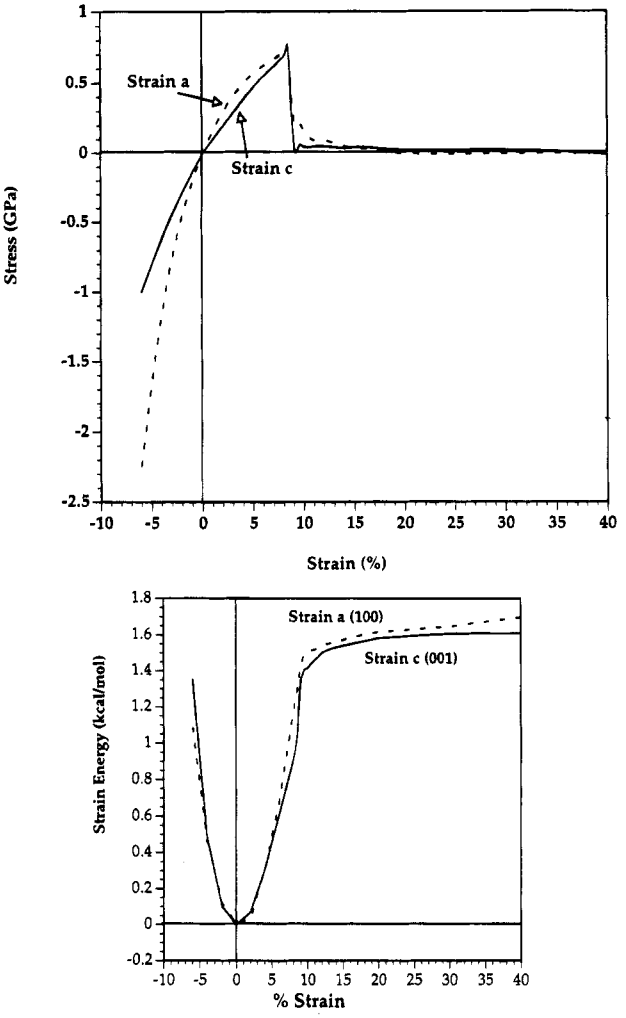

Figure 5. (a, top) Calculated stress−strain curves for crystalline P(SiH) in directions perpendicular to the chain axis. (b, bottom) Strain energy (kcal/mol) as a function of strain.

the experimental frequencies (Table 15) than our packed P(SiH) frequencies. This may be because the samples are not very crystalline (including silicon-like clusters and metastable gauche configurations), leading to an inefficiently packed local structure better approximated by a single chain.

Figure 4 shows the phonon dispersion curves for the all-trans polysilane crystal (there are no experimental numbers). The low energy bands depend strongly upon the van der Waals and Coulombic interactions as well as the torsional force constant. In the case of PE (Karasawa et al.[11a]) the MSXX led to average errors of 7.9 cm^{-1} for n-C_4H_{10} and 24 cm^{-1} for the crystal. The MSXX FF reproduces the vibrational frequencies of n-Si_4H_{10} with an error of 6 cm^{-1}, but we expect larger errors for the crystal.

Figure 5a shows stress−strain curves for stresses along the unit cell axes (perpendicular to the chain). In these calculations we used a supercell consisting of 32 primitive cells. Although the Young's moduli perpendicular to the chain direction are larger for P(SiH) than for PE, the yield stress is similar. This is the result of the higher anharmonicity of the P(SiH) nonbond interactions, which fall off faster than those of PE. In the case of PE, shear perpendicular to the chain direction eventually leads to a transition to a metastable monoclinic phase. Shearing P(SiH) using our FF did not lead to any stable phases. Minimization from any structure arrived at by shearing always led back to the orthorhombic unit cell.

The surface energy is calculated by stretching the crystal perpendicular to the surface until the crystal breaks (Figure 5b).

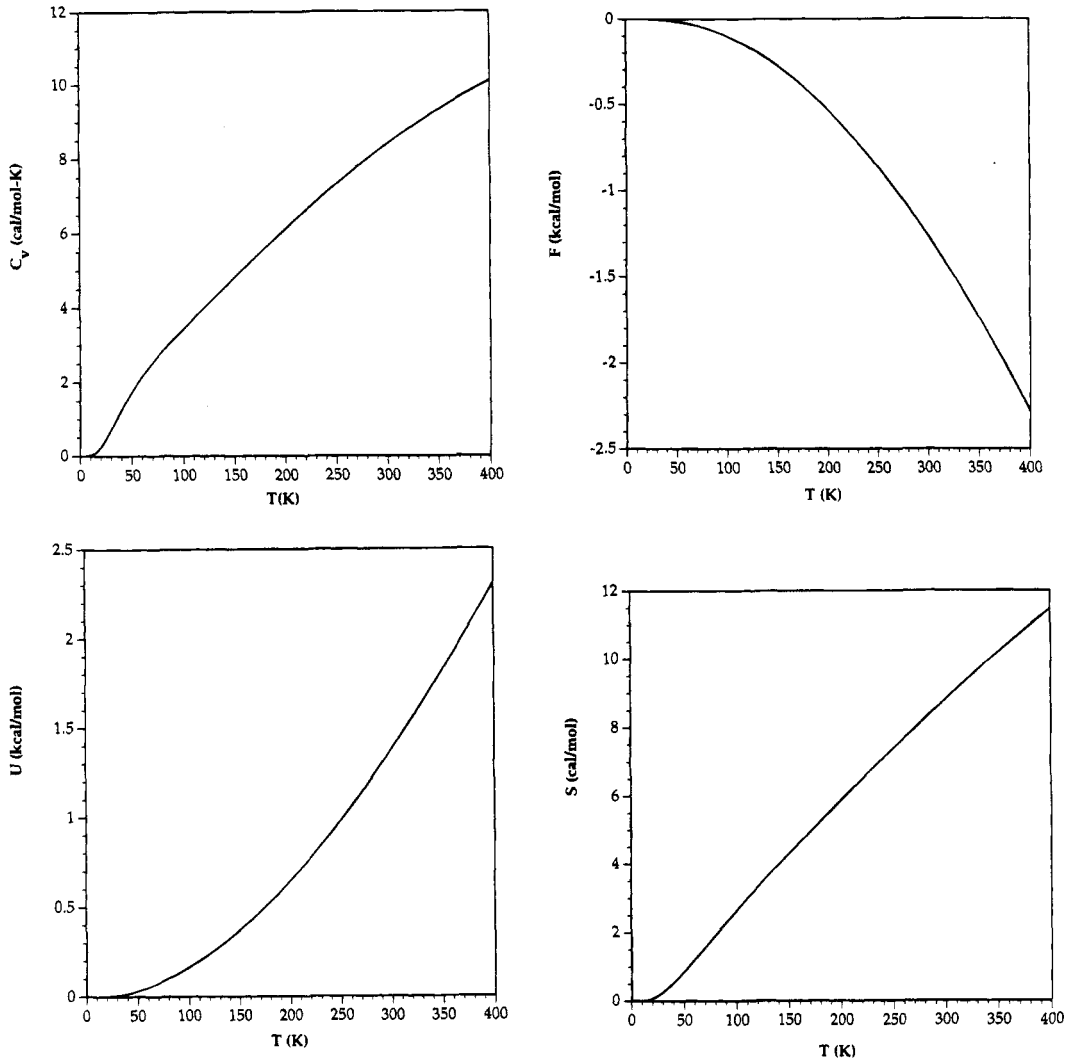

Figure 6. Thermochemical properties as a function of temperature (using a 5 × 5 × 5 grid of phonons in the Brillouin zone): (a, top left) head capacity (C_v); (b, top right) Helmholtz free energy; (c, bottom left) internal energy; (d, bottom right) entropy.

From the curves in Figure 5 we derive surface energies of 63.5 dyn/cm for the (100) surface and 66.9 dyn/cm for the (001) surface (using a conversion factor of 694.8 to convert from kcal/(mol·Å^2) to erg/cm^3). This compares with 106.8 dyn/cm (100) and 109.2 dyn/cm (001) for the analogous surfaces of polyethylene. The (100) surface has two SiH_2 groups per unit cell, leading to a surface energy per SiH_2 of 1.698 kcal/mol while the (001) surface has four SiH_2 groups per unit cell leading to a surface energy of 1.609 kcal/mol. This compares with 0.938 and 0.720 kcal/mol for the analogous surfaces of polyethylene. We know of no experimental information on such properties for P(SiH). Assuming only nearest-neighbor fiber−fiber interactions, we would expect a surface energy of one-third the cohesive energy of the crystal. This would predict a surface energy of 1.42 kcal/mol for both the (100) and (001) surfaces, which is low by ≈15%.

Figure 6 shows the predicted heat capacity (C_v), entropy, enthalpy, and free energy versus temperature (again, we know of no experimental data).

V. Summary

In this paper we develop the MSXX FF for P(SiH) that should be accurate and useful for a variety of structural, thermodynamic, spectroscopic, mechanical, and surface properties. The method follows the procedure developed by Karasawa et al.[11a] for PE (modified for incomplete experimental vibrational data). For PE the substantial amount of data on experimental properties validated the accuracy attained with this procedure. For P(SiH), sample quality is poor and this procedure is used to predict the properties of crystalline P(SiH) in advance of experiment.

Spectroscopic force fields (SFF) usually omit the electrostatic (Q) and van der Waals (vdW) nonbond terms since the geometry is considered fixed. For MD calculations the FF must describe how the energy changes with geometry, and hence the MSXX FF includes these intramolecular nonbond terms. They are small for P(SiH) oligomers except for torsional modes, where they make significant contributions. On the other hand, the bulk properties of P(SiH) depend greatly on the intermolecular interactions.

The HBFF[6] combines experimental vibrational frequencies with the normal mode description of the vibrations from *ab initio* calculations. For P(SiH) oligomer systems it was necessary to extend the HBFF approach to handle systems with incomplete spectroscopic information through scaling.

The validity of the resulting MSXX FF is tested by calculating the properties for *n*-Si_5H_{12}, where we find the modes to be within 2% of the scaled *ab initio* (HF/6-31G**) results (no experimental data are available). MSXX predicts a SiSiSi bond angle 1.1° larger than HF, which will lead to a slightly too large bond angle for the crystal. Despite the slight difference in the geometry, the MSXX predicts the vibrational frequencies accurately.

The MSXX predictions should be useful for predicting the spectra of larger oligomers where assignments are incomplete (particularly for torsional modes and skeletal modes) and for the P(SiH) condensed phase where there are no assignments.

We used the Nosè formalism[19] of canonical MD to extract thermodynamic properties of polysilane from the MD simulations. Properties at various temperatures were averaged from dynamics calculations, and thermal expansion coefficients were derived for temperatures up to 450 K. Other properties were calculated using the unit cell at the desired temperature.

Acknowledgment. The research was funded by NSF (ASC 9217368). The facilities of the MSC are also supported by grants from DOE-AICD, NSF-CHE, Allied Signal, Asahi Chemical, Asahi Glass, BP America, Chevron Petroleum Technologies Co., BF Goodrich, Teijin Ltd., Xerox, Vestar, Hughes Research Laboratories, and Beckman Institute.

References and Notes

(1) Miller, R. D.; Michl, J. *Chem. Rev.* **1989**, *89*, 1359, and references cited therein.

(2) Damewood, J. R., Jr.; West, R. *Macromolecules* **1985**, *18*, 159.

(3) Zeigler, J. M. *Synth. Met.* **1989**, *28*, C581.

(4) Mintmire, J. W. *Phys. Rev. B* **1989**, *39*, 13350.

(5) Cui, C. X.; Kertesz, M. *Macromolecules* **1992**, *25*, 1103.

(6) Dasgupta, S.; Goddard, W. A., III. *J. Phys. Chem.* **1989**, *90*, 7207.

(7) Mayo, S. L.; Olafson, B. D.; Goddard, W. A., III. *J. Phys. Chem.* **1990**, *92*, 7488.

(8) Frisch, M. J.; Trucks, G. W.; Head-Gordon, M.; Gill, P. M. W.; Wong, M. W.; Foresman, J. B.; Johnson, B. G.; Schlegel, H. B.; Robb, M. A.; Replogle, E. S.; Gomperts, R.; Andres, J. L.; Raghavachari, K.; Binkley, J. S.; Gonzalez, C.; Martin, R. L.; Fox, D. K.; Defrees, D. J.; Baker, J.; Stewart, J. J. P.; Pople, J. A. *Gaussian 92 Revision*, Gaussian, Inc.: Pittsburgh, PA, 1992.

(9) PS-GVB: Ringnalda, M.; Langlois, J.-M.; Greeley, B. H.; Russo, T. V.; Muller, R. P.; Marten, B.; Won, Y.; Donnelly, R. E., Jr.; Pollard, W. T.; Miller, G. H.; Goddard, W. A., III; Friesner, R. A. *PS-GVB*, v1.03; Schroedinger, Inc.: 1994. Ringnalda, M. N.; Won, Y.; Friesner, R. A. *J. Chem. Phys.* **1990**, *93*, 3397. Langlois, J.-M.; Muller, R. P.; Coley, T. R.; Goddard, W. A., III; Ringnalda, M. N.; Won, Y.; Friesner, R. A. *J. Chem. Phys.* **1990**, *92*, 7488.

(10) Chirlian, L. E.; Francl, M. M. *J. Comput. Chem.* **1987**, *8*, 894.

(11) (a) Karasawa, N.; Dasgupta, S.; Goddard, W. A., III. *J. Phys. Chem.* **1991**, *95*, 2260. (b) Fogarasi, G.; Pulay, P. *Vibrational Spectra and Structure*; Elsevier: New York, 1985; Vol. 14, p 125.

(12) Cremer, D.; Binkley, J. S.; Pople, J. A.; Hehre, W. J. *J. Am. Chem. Soc.* **1974**, *96*, 6900.

(13) McMurray, H. L.; Solbrig, A. W., Jr.; Boyter, J. K.; Noble, C. *J. Phys. Chem. Solids* **1967**, *28*, 2359.

(14) Yamasaki, T.; Dasgupta, S.; Goddard, W. A., III. *J. Chem. Phys.*, submitted for publication.

(15) Kattenberg, H. W.; Oskam, A. *J. Mol. Spectrosc.* **1974**, *49*, 52.

(16) Durig, J. R.; Church, J. S. *J. Chem. Phys.* **1980**, *73*, 4784.

(17) McKean, D. C. *Spectrochim. Acta* **1992**, *48A*, 1335.

(18) Feher, F.; Fisher, H. *Naturwissenschaften* **1969**, *51*, 461.

(19) (a) Cagin, T.; Goddard, W. A., III; Ary, M. L. *J. Comp. Polym. Phys.* **1991**, *1*, 241. (b) Cagin, T.; Karasawa, N.; Dasgupta, S.; Goddard, W. A., III. *Mater. Res. Soc. Symp. Proc.* **1992**, *278*, 61. (c) Nosé, S. *J. Chem. Phys.* **1984**, *81*, 511. (d) Parrinello, M.; Rahman, A. *J. Appl. Phys.* **1981**, *52*, 7182.

(20) POLYGRAF is from Molecular Simulations Inc., Burlington, MA.

JP950293W